Chapter 17
Role of LTD in Cerebellar Motor Learning: The 75th FUJIHARA Seminar "The Cerebellum as a CNS Hub"

Kazuhiko Yamaguchi

17.1 Introduction

Elaborated machine-like neuronal circuit of the cerebellar cortex was revealed 50 years before (Eccles et al., 1967), but its functional interpretation was elusive at that time. Two years later, Marr proposed that this neuronal circuit could work as a learning machine. He proposed a Hebbian-type synaptic plasticity at PF-PC synapse, namely, the synapses from parallel fibers to Purkinje cells were facilitated by the conjunction of presynaptic and climbing fiber (or postsynaptic) activity (Marr, 1969). On the other hand, Albus claimed that in order for the learning process to be stable, pattern storage must be accomplished principally by weakening synaptic weights rather than by strengthening them (Albus, 1971). Ten years later, by means of in vivo recording from rabbit cerebellum, Ito's group experimentally found that the conjunction of PF and CF stimulation induced long-term depression (LTD) of synaptic transmission at PF-PC synapse (Ito et al., 1982). Then, this theory was called as Marr-Albus-Ito's theory of the cerebellar cortex.

The molecular mechanism of LTD was investigated using new in vitro experimental preparations, such as a cerebellar slice (Sakurai, 1987) and cultured cerebellar neurons (Hirano & Ohmori, 1986; Linden & Conner, 1991). Briefly, repetitive firing of PF activates not only AMPA-type glutamate receptor (AMPA-R) but also mGluR1 located at the periphery of postsynaptic region of dendritic spine of PC. Activated mGluR1, coupled with $\alpha_{q/11}$ of GTP-binding protein, activates PLCβ, and then IP_3 and DG were produced. IP_3 bound to IP_3 receptor 1(IP_3R1) of

K. Yamaguchi (✉)
Center for Brain Science, RIKEN, Saitama, Japan

Department of Ultrastructural Research, National Institute of Neuroscience, NCNP, Tokyo, Japan
e-mail: kazuhiko.yamaguchi@ncnp.go.jp

H. Mizusawa, S. Kakei (eds.), *Cerebellum as a CNS Hub*,
Contemporary Clinical Neuroscience, https://doi.org/10.1007/978-3-030-75817-2_17

the endoplasmic reticulum (ER) and released Ca^{2+} from ER. Action potential of CF activates P/Q-type voltage-gated Ca^{2+} channel (VGCC) at PC's dendritic region. Ca^{2+} influx through P/Q Ca^{2+} channel sensitizes IP_3R1 sensitivity to IP_3, then Ca^{2+} release from ER is robustly enhanced, and conjunctive activation of VGCC and mGluR-IP_3 pathways increases $(Ca^{2+})_{in}$ more than an additive level in the dendritic spine (Wang et al., 2000; Kakegawa et al., 2018). This synergistic increase in $(Ca^{2+})_{in}$ activates PKCα, and activated PKCα phosphorylates Ser880 at GluA2 C-terminus. This phosphorylation of Ser880 requires in advance dephosphorylation of Tyr876 by megakaryocyte protein phosphatase (PTPMEG), bound to cytoplasmic terminus of GluR delta 2 (Kohda et al., 2013). Then, AMPA-Rs containing phosphorylated GluA2 are detached from the scaffold protein and internalized with PICK1 in AP2- and clathrin-dependent manners (Wang & Linden, 2000; Kakegawa et al., 2018).

To correlate LTD and motor learning, gene-manipulated animals provided advantageous systems. Gene deletion of mGluR1 caused both deficiency of LTD and conditioned eyeblink (Aiba et al., 1994). In mice lacking Gαq, both LTD and motor coordination were impaired (Hartmann et al., 2004). In PLCβ4-deficient mice, LTD was impaired in rostral cerebellum (lobes 1–6) (Hirono et al., 2001; Miyata et al., 2001), and delay eyeblink conditioning was severely impaired (Kishimoto et al., 2001). Transgenic mouse expressing pseudosubstrate PKC inhibitor only in Purkinje cell showed complete blockade of LTD induction and absence of ability to adapt their vestibulo-ocular reflex (VOR) gain during visuo-vestibular training (De Zeeuw et al., 1998). In GluR delta 2-deficient mice, both LTD and motor coordination were impaired (Kashiwabuchi et al., 1995). Also GluR delta 2 mutant mice failed to change the VOR or optokinetic response (OKR) gain adaptively in response to sustained vestibular and/or visual stimulation (Katoh et al., 2005).

Accordance between impairment of LTD and motor learning in these gene-manipulated animals supported the idea that LTD was the mechanism of the motor learning. Recently, however, discrepancies between LTD and motor learning have been reported in mice with a mutation that targeted the expression of PF-PC LTD by blocking AMPA-R internalization regulated via the phosphorylation of AMPA-Rs. In these mice, motor learning behavior was normal, but no PF-PC LTD was observed (Schonewille et al., 2011). However, the induction of LTD was only attempted using one type of protocol at room temperature. We reexamined slices obtained from these GluA2 K882A and GluA2 Δ7 knock-in mutants at 3–6 months of age. Several types of LTD-inducing protocols at higher temperature were used, and LTD-inducing ability was detected in both types of knock-in mutants (Yamaguchi et al., 2016). These new standard protocols would be necessary especially to detect compensated LTD in mutant animals.

17.2 Materials and Methods

17.2.1 Animals

The knock-in (KI) mice (GluR2K882A and GluR2Δ7) (Fig. 17.1a), which were gifts from R.L. Huganir (Steinberg et al., 2006). Sperms were obtained from both KI mice by ectomy and used for in vitro insemination of oocytes from C57BL/6

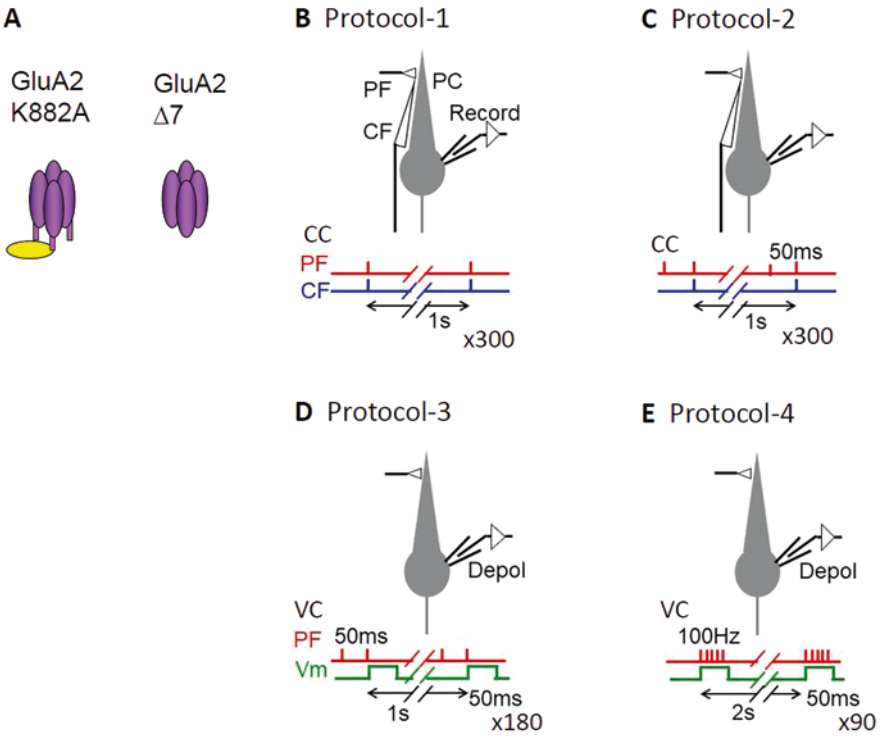

Fig. 17.1 Two types of mutated GluA2 and schematic illustration of LTD-inducing protocols 1–4. (**a**) Mutation of K882 within the intracellular C-terminus of the GluA2 subunit (GluA2 K882A) and the absence of the C-terminal 7 amino acids of GluA2 (GluAΔ7). PKCα cannot phosphorylate S880 of GluA2 K882A, but PIK1 can bind to C-terminus of GluA2 K882A. (**b**) Protocol 1 conjunctive stimulation. 1PF and 1CF stimuli are applied simultaneously 300 times at 1 Hz (5 min) under current-clamp conditions. Electrode for whole-cell recording contains K^+-based internal solution. (**c**) Protocol 2 conjunctive stimulation. 2PF and 1CF stimuli are applied simultaneously 300 times at 1 Hz (5 min) under current-clamp conditions. Electrode contains K^+-based internal solution. (**d**) Protocol 3 conjunctive stimulation. 2PF and somatic depolarization (−70 to 0 mV, 50 ms) are applied 180 times at 1 Hz (3 min) under voltage-clamp conditions, so that the second PF stimulus is applied simultaneously with the beginning of the somatic depolarization. Electrode contains Cs^+-based internal solution. (**e**) Protocol 4 conjunctive stimulation. 5PF at 100 Hz and somatic depolarization are applied 90 times at 0.5 Hz (3 min) under voltage-clamp conditions, simultaneously. Electrode contains Cs^+-based internal solution

mice. The offspring from the fertilized oocytes was proliferated by backcrossing to C57BL/6 mice and then by crossbreeding to obtain homozygous KI mice. Genotypes were determined by PCR amplification of tail DNA samples followed by digestion with restriction enzymes for which unique sites had been engineered (GluR2Δ7, Bgl II; GluR2K882A, Bsl I) (Steinberg et al., 2006). The primers used were Glu L (5'-AACGAATGAAGGTGGCAAAG-3′) and Glu R (5'-AAGAGCTTAAGGACGCGACA-3′). Genotypes were confirmed by second-round genotyping on genomic DNA purified from mouse brain slices used for electrophysiological recording. Mice were kept in the animal facility of RIKEN Brain Science Institute under well-controlled living conditions.

17.2.2 Electrophysiological Studies

All procedures involving animals were approved by the RIKEN committee on the care and use of animals in experiments. Both male and female wild-type mice (C57BL/6, 3–6 months) were used.

All solutions should be made in ultrapure water with free of metals and other impurities. Working artificial cerebrospinal fluid (ACSF) for slice-cutting and recording are made freshly on the day of experiment from a 10 times (x10) stock of ACSF. Bubble the solutions with 5% CO_2/95% O_2 gas mixture before use. The pH of ACSF is adjusted to 7.4 ± 0.1, and osmolarity is adjusted to 315 ± 5 mOsm/kg by adding ultrapure water. ACSF is containing (in mM) 125 NaCl, 3 KCl, 2 $CaCl_2$, 1 $MgSO_4$, 1.25 NaH_2PO_4, 26 $NaHCO_3$, and 20 glucose. For slice-cutting, 50 μl of tetrodotoxin (TTX) (1 μM) was added into the ice-cold ACSF. Using the linear slicer, sagittal slices of vermis were cut with thickness of 300 μm. Slice was used after incubation at 26 °C for, at least, 1 h.

The recording chamber was perfused with oxygenated ACSF containing 100 μM picrotoxin at a rate of 2 ml/min and maintained at 30.0 ± 1.0 °C. The volume of the perfusion bath was 0.5 ml. Whole-cell slice-patch recordings of PCs were performed under an upright microscope with x40 water immersion objective. Patch pipettes were made from borosilicate tubings and filled with a solution containing the following (in mM) (resistance, 2–4 MΩ): for the K^+-based internal solution, 60, KCl; 60, K-gluconate; 0.3, EGTA; 4, $MgCl_2$; 4, ATP; 0.4, GTP; and 30, HEPES (pH 7.2) and, for the Cs^+-based internal solution, 60, CsCl; 40, D-gluconate; 20, TEA-Cl; 0.3, EGTA; 4, $MgCl_2$; 4, ATP; 0.4, GTP; and 30, HEPES (pH 7.2, adjusted using CsOH). Whole-cell recordings were performed using a patch-clamp amplifier (MultiClamp 700A). Recorded signals were filtered at 3 KHz and digitized at 10 KHz. Stimulation and online data acquisition were performed using pCLAMP 9 software (Molecular Devices). Access resistance and input resistance were constantly monitored by applying a small hyperpolarizing voltage step (2 mV, 100 ms). PFs in the molecular layer or CFs in the granule cell layer or molecular cell layer were focally stimulated by applying pulses (duration, 0.1 ms) to a slice through a glass pipette (tip diameter, 5–10 μm) positioned on the surface of a cerebellar slice.

The membrane potential was held at −65 or − 75 mV, and a PF-evoked PF-EPSC was evoked at a frequency of 0.1 Hz as a test response.

17.2.3 LTD-Inducing Protocols

Four protocols were used to induce LTD. In protocol 1 and protocol 2, PF and CF were stimulated under current-clamp condition, and in protocol 3 and protocol 4, PF stimulation and somatic depolarization were applied under voltage-clamp condition. Schematic diagrams of protocols 1–4 are shown in Fig. 17.1b–e. In protocol 1 or 2, after switching to the current-clamp mode, LTD was induced by a protocol composed of 300 single (protocol 1) or double (protocol 2) PF stimuli in conjunction with CF stimuli. In the double PF stimuli protocol, the first PF stimulus was followed by a 50 ms interval by a CF stimulus and the second PF stimulus. During the PF-CF conjunctive stimulation, no DC was applied except when there was the need to prevent spontaneous firing. The resting membrane potential was varied between −50 and − 60 mV. Under the voltage-clamp condition using a recording electrode containing the Cs^+-based internal solution, two (protocol 3) or five (protocol 4) PF stimuli were applied repeatedly at 1 or 0.5 Hz for 3 min, respectively, coupled with a depolarizing pulse for 50 ms from a holding potential of −75 mV to a potential (0 to +40 mV) at which a few inward current surges were observed, probably representing the generation of dendritic Ca^{2+} spikes.

Statistics To evaluate statistical significances of data between the experimental group and the control group, the *t*-test was used. On the other hand, the statistical significance of intergroup differences among the three genotypes was tested by one-way ANOVA and the Tukey-Kramer post hoc test. Data are represented as mean ± SEM (cell number of tested PCs).

17.3 Results

The two types of mutant, GluA2 K882A and Δ7 KI mice, examined in this study showed seemingly normal daily behavior. Acute slices of cerebellar vermis were obtained from them at 3–6 months of age where motor learning capability was fully developed (Schonewille et al., 2011). Whole-cell recording from PCs under the voltage- or current-clamp condition showed virtually normal features of membrane resistance and PF-EPSCs, simple spikes, and complex spikes in the mutant slices as compared with the wild type (WT). In WT, all types of conjunctive stimulation (protocols 1 to 4) caused LTD, which continued for more than 1 h, but for convenience, the magnitude of LTD was estimated by measuring the amplitude of the depressed PF-EPSC peak at 26–30 min after the onset of conjunctive stimulation, relative to their mean amplitude measured during the 5 min preconjunction period.

Four types of protocols were used in this study to induce cerebellar LTD. In the first two protocols (protocols 1 and 2), conjunction of PF stimulation and CF stimulation was applied under current-clamp condition. In the other two protocols (protocols 3 and 4), CF stimulation was replaced by somatic depolarization under voltage-clamp condition.

Protocol 1 Conjunction of one PF stimulation and one CF stimulation under current-clamp condition was conventionally used in slice preparation (Koekkoek et al., 2005). The shape of complex spike elicited by conjunctive stimulation was similar to that elicited by CF stimulation alone, with the first steep spikelet followed by two to three spikelets (Fig. 17.2a). Firstly, a single-shock stimulus (0.1 ms in duration) was applied to PFs in combination with a single stimulus simultaneously applied to CF and repeated at 1 Hz for 5 min (300 pulses) (Fig. 17.1a). This protocol 1 was used previously as effective in inducing LTD (Karachot et al., 1994; Schonewille et al., 2011). In the present study, protocol 1 was effective in inducing LTD in WT PCs (75.6 ± 4.0%, $n = 6$, $p = 0.002$, *t*-test) (Fig. 17.2b), but not in Δ7 PCs (103.9 ± 9.6, $n = 6$, $p = 0.898$) (Fig. 17.2d). K882A PCs may appear to exhibit a modest LTD, which, however, is not statistically significant in its magnitude (86.0 ± 7.2, $n = 6$, $p = 0.228$) (Fig. 17.2c). Thus, protocol 1 was effective in inducing LTD only in WT, but not in either K882A or Δ7 PCs (Fig. 17.1e), which is in agreement with the report by Schonewille et al. (2011).

Protocol 2 PFs were stimulated twice at 50 ms intervals, and the second PF stimulus was synchronized with a single CF stimulus (Fig. 17.1c). Similar shape of complex spike was observed during stimulation with protocol 1 (Fig. 17.3a). PF stimulation with 2 pulses was expected to release more Glu and to activate mGluR1 more robustly, because mGluR1 is located at the marginal zone of the synaptic region (Masugi-Tokita et al., 2007). This (2PF + CF) conjunctive stimulation induced significant LTD in K882A PCs (81.0 ± 3.4, $n = 6$, $p = 0.008$) (Fig. 17.3c) comparable to that in WT PCs (82.8 ± 4.95%, $n = 6$, $p = 0.036$) (Fig. 17.3b), there being no statistically significant difference between them ($p = 0.957$, Tukey-Kramer test). However, no LTD was induced in Δ7 PCs (94.8 ± 5.1, $n = 6$, $p = 0.351$) (Fig. 17.3d). Thus, protocol 2 was effective in inducing LTD in both WT and K882A, but not in Δ7 PCs (Fig. 17.3e).

To ensure that protocol 1- and protocol 2-evoked LTD is specifically induced by conjunctive stimulation of PF and CF and not by PF or CF stimulation alone, we tested the effect of applying CF stimuli alone in place of PF-CF conjunctive stimulation. No significant change in EPSC amplitude during 25–29 min was observed in any of the three PC groups, WT PCs (101.1 ± 1.5%, $n = 3$, $p = 0.41$, *t*-test), K882A PCs (100.5 ± 3.9%, $n = 3$, $p = 0.90$), and Δ7 PCs (102.2 ± 2.8, $n = 3$, $p = 0.48$), as plotted in Figs. 17.2b–d and 17.3b–d as control for conjunctive stimulation. Application of PF alone in place of PF-CF conjunction was shown previously to induce no LTD in WT, K882A, or Δ7 PCs (Schonewille et al., 2011). In this study, we also observed that PF or 2PF induced no LTD, but often long-term potentiation (LTP), as has been known (Schonewille et al., 2011; Lev-Ram et al., 2002).

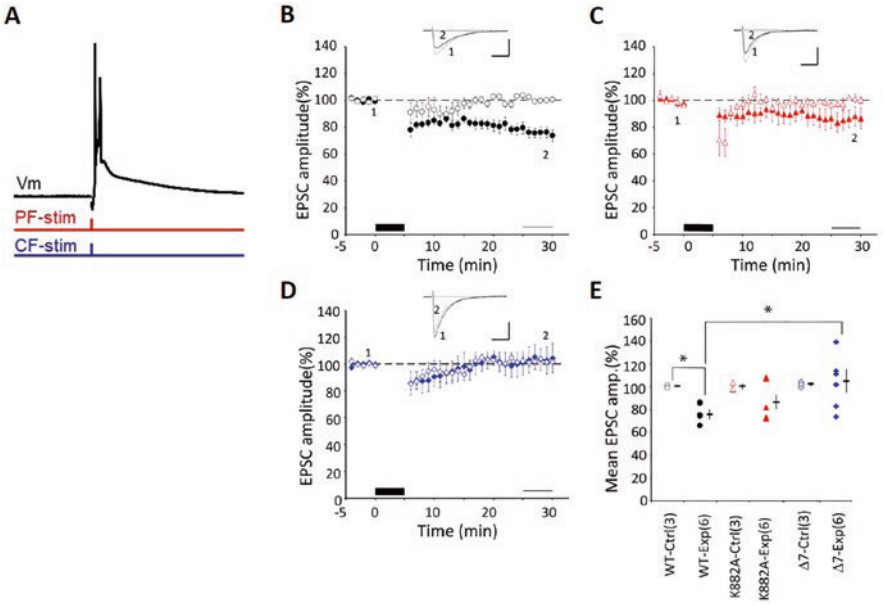

Fig. 17.2 LTD induction by protocol 1 conjunctive stimulation. (**a**) Membrane potential traces of PC elicited by protocol 1 conjunctive stimulation. (**b**) Mean PF-EPSC amplitude recorded from WT PCs before and after protocol 1 conjunctive stimulation (black column at bottom). The horizontal thin line (bottom) indicates the period of 25–29 min after conjunctive stimulation onset, where the amplitudes of PF-EPSCs were compared to estimate LTD. PF-EPSC amplitude was normalized by those recorded before conjunctive stimulation. Filled symbols indicate the mean amplitude of the experimental group. Open symbols indicate the PF-EPSC amplitude of the control group, in which only CF stimulation was applied in place of conjunctive stimulation. Error bars denote SEM. *Inset*: superposed PF-EPSC traces (top) recorded before (marked 1) and 25–29 min after conjunctive stimulation onset (marked 2). Each trace represents the average of six records. *Bars*: 100 ms, 150 pA. (**c**) Similar to **b** but for K882A PCs. (**d**) Similar to **b**, but for Δ7 PCs. (**e**) Summary plot of mean PF-EPSC amplitude recorded during 25–29 min after onset of conjunctive stimulation in WT, K882A, or Δ7 mice. Filled symbols are plots for the test with protocol 1, whereas open symbols are plots for the control measurement where conjunctive stimulation was replaced by 1CF stimulation. The mean and SEM of each group are indicated by a horizontal rod and vertical bar, respectively. Numbers in parentheses represent cell number. $^*p < 0.05$. Intragroup comparison, *t*-test. Intergroup comparison, ANOVA and post hoc Tukey-Kramer test

For the LTD induced by protocol 1 and 2, EPSC amplitude measured during 25–29 min after onset of conjunctive stimulation was widespread. The shape of complex spike was variable from cell to cell. Because the spikelets within the complex spike reflected Ca channel activation (De Schutter & Bower, 1994), whether the shape of complex spike affected LTD amplitude was examined. Relation between sum of voltage peaks 1–4 (Fig. 17.4a) and LTD amplitude in protocol 1 was compared, but there is no correlation ($r = -0.03$) (Fig. 17.4b). Because the first spikelet represents mainly Na component and spikelets 2–4 contain more of the Ca^{2+} component (Swensen & Bean, 2003), the relation between sum of voltage

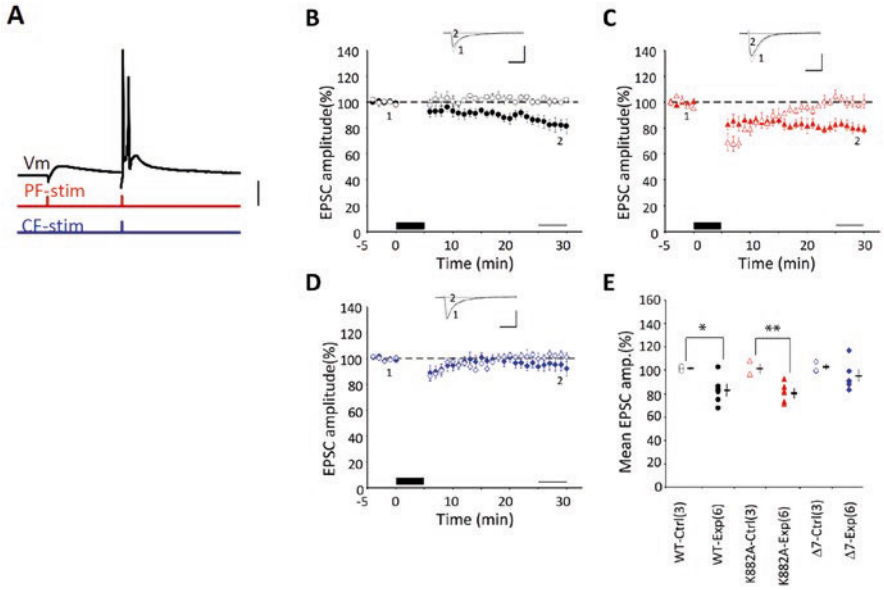

Fig. 17.3 LTD induction by protocol 2 conjunctive stimulation. (**a**) Membrane potential traces of PC elicited by protocol 2 conjunctive stimulation. (**b–e**) Similar to Fig. 17.2b–e, but for conjunction protocol 2, where 2PF and 1CF stimulations were applied conjunctively at 1 Hz for 5 min under current-clamp conditions. In **E**, * $p < 0.05$, ** $p < 0.01$, *t*-test

peaks 2–4 and LTD amplitude was analyzed, and moderate correlation was detected ($r = 0.67$) (Fig. 17.4c). Next, voltage trace of the complex spike was differentiated (Fig. 17.4d), and sum of maximum rate of rises (MRRs) of each spikelet was calculated, and then sum of the MRRs was multiplied by value of each PC's Cm, and this product gave approximate measure of the Ca^{2+} current of each PC during complex spike (Fukuda et al., 1981). Relation between Cm x summed MRRs of spikelets 1–4 and amplitude of LTD was plotted (Fig. 17.4e), but no correlation was detected ($r = 0.17$). The relation between Cm × sum of MRRs of spikelets 2–4 and LTD amplitude showed weak correlation ($r = 0.36$) (Fig. 17.4f).

Protocol 3 Under voltage-clamp condition using Cs^+-based internal solution, conjunction of 2PF stimulation and somatic depolarization were applied (Fig. 17.1d). The somatic depolarization was applied 50 ms after the initial PF stimulation, and the second PF stimulation was applied simultaneously with the beginning of the somatic depolarization. Inward current was elicited upon somatic depolarization from −70 to 0 mV. Tail current was also evoked after repolarization. Sometimes, repetitive generation of inward current was observed, which would reflect Ca^{2+} spike activity at the remote dendritic region where the membrane potential was not clamped sufficiently, in spite of using Cs^+-based internal solution (Fig. 17.5a) (Steinberg et al., 2006). The patch pipette was filled with a Cs^+-based internal solution to improve space clamping along PC dendrites by blocking K^+channels. The

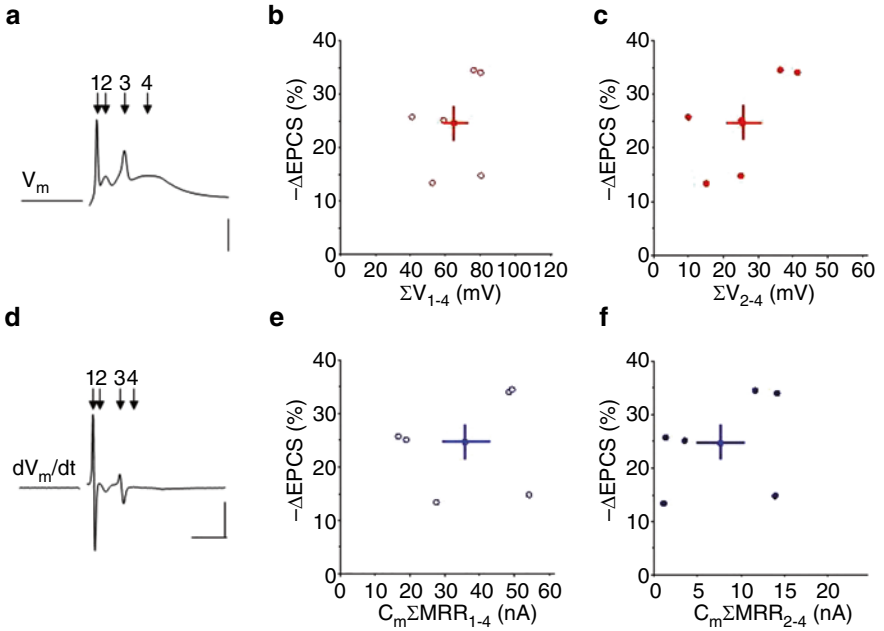

Fig. 17.4 Relationship between spikelet of a complex spike and LTD amplitude. (**a**) Representative trace of a complex spike elicited by protocol 1. Arrows indicate peaks of spikelets (1–4). Bar: 20 mV. (**b**) Relationship between the sum of the amplitude of spikelets (1–4) and LTD amplitude (-ΔEPSC %) ($r = -0.03$). (**c**) Relationship between the sum of the amplitude of spikelets (2–4) and LTD amplitude ($r = 0.67$). (**d**) Representative trace of differentiated complex spikes shown in A. Arrows indicate peaks of dV_m/dt of spikelets. Bars: 5 ms, 50 V/s. (**e**) Relationship between products of the Cm and the sum of the MRR of spikelets (1–4) and amplitude of LTD (-ΔEPSC %) ($r = 0.17$). (**f**) Relationship between the product of the Cm and the sum of the MRR of spikelets (2–4) and amplitude of LTD ($r = 0.36$)

mean **Rm** in cells recorded with the pipette containing the Cs^+-based internal solution was 3–4 times larger than those recorded with a pipette containing a K^+-based solution. This maneuver is expected to ensure efficient activation of voltage-dependent Ca^{2+} channels located at dendritic regions, where PFs form synapses on PCs. With this protocol 3, LTD was induced in WT PCs (64.9 ± 4.3%, $n = 5$, $p = 0.0007$), K882A PCs (72.0 ± 3.8, $n = 7$, $p = 0.003$), and Δ7 PCs (80.0 ± 7.2, $n = 6$, $p = 0.026$) (Fig. 17.5b–d). No significant difference was found between these three groups ($p = 0.151$, one-way ANOVA) (Fig. 17.5e).

Protocol 4 Five PF stimuli at 100 Hz were given simultaneously with the somatic depolarization under voltage-clamp condition (Fig. 17.1e). Repetitive generation of inward current was elicited during depolarization, and tail current was elicited after the repolarization. Timing of repetitive generation of the inward current was not synchronized with PF stimuli (Fig. 17.6a). Sometimes, repetitive generation of the inward current continues after repolarization. This (5PF + Depo) conjunctive stimulation (protocol 4) was effective for inducing LTD in WT PCs (76.0 ± 6.8%,

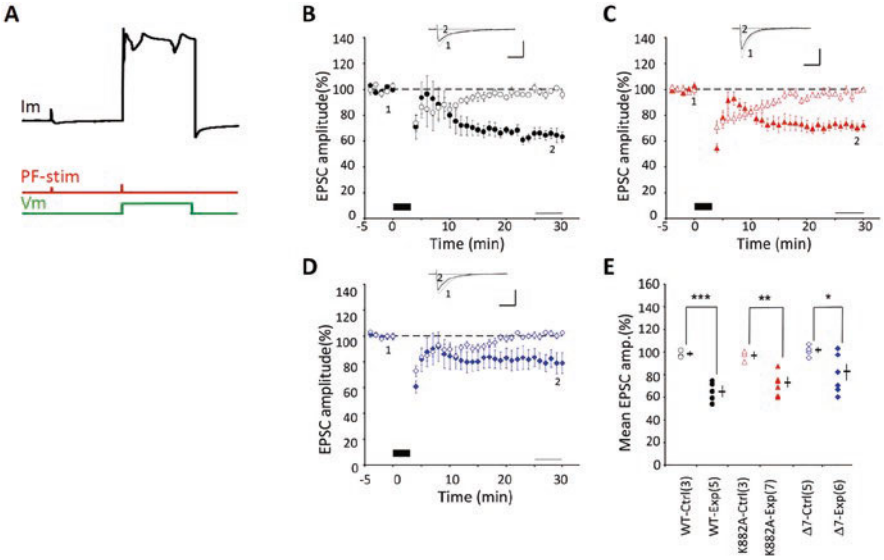

Fig. 17.5 LTD induction by protocol 3 conjunctive stimulation. (**a**) Membrane current traces of PC elicited by protocol 3 conjunctive stimulation. (**b–e**). Similar to Fig. 17.2**b–e**, but for conjunction protocol 3, where 2PF stimulation and one depolarizing pulse were applied conjunctively at 1 Hz for 3 min under voltage-clamp conditions. In **E**, * $p < 0.05$, ** $p < 0.01$, *** $p < 0.001$, *t*-test

$n = 3$, $p = 0.031$), K882A PCs (71.0 ± 2.0%, $n = 4$, $p = 0.00017$), and Δ7 PCs (70.7 ± 7.4%, $n = 3$, $p = 0.013$) (Fig. 17.6b–d). No statistically significant difference was found among the three groups ($p = 0.749$, one-way ANOVA) (Fig. 17.6e). With protocol 3 and protocol 4, CF stimulation was replaced with depolarizing pulses that caused Ca^{2+} entry, which was similar to that evoked by CF responses. As control experiment, we applied 50 ms depolarizing pulses at 1 Hz for 3 min separately from PF stimuli. These depolarizing pulses induced short-term depression lasting for 20 min but did not cause LTD in any of the three PC groups (Figs. 17.5 and 17.6).

Protocol 4 was originally used for young wild-type mouse (P14–21) (Steinberg et al., 2006). They reported that LTD was induced by 30 conjunctive stimulations at 0.5 Hz at RT in wild type, but in neither K882A nor Δ7 PCs (Steinberg et al., 2006). However, when 30 conjunctive stimulations were applied to adult wild-type cerebellar slice (3–6 months) at 30 °C, no LTD was induced (Fig. 17.7a, c). In contrast, when 90 conjunctive stimulations were applied, usual amplitude of LTD was observed in wild type (Fig.17.7b, c). Again, somatic depolarization alone (90 times at 0.5 Hz) did not induce LTD (Fig. 17.5b).

PKCα inhibitor sensitivity It may be questioned whether the LTD induced by replacing CF stimuli with depolarization in protocol 3 or protocol 4 shares a common signal transduction mechanism with the LTD induced by PF-CF conjunctive stimulation in protocol 1 and protocol 2. To test this, we chose Gö6976, a potent PKCα inhibitor, which has been shown to play a crucial role in LTD induction (Xia

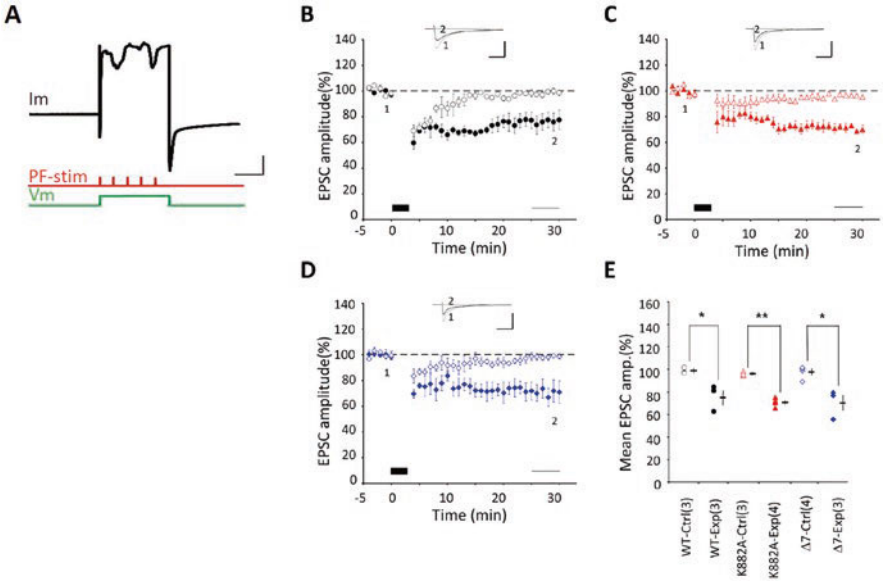

Fig. 17.6 LTD induction by protocol 4 conjunctive stimulation**.** (**a**) Membrane current trace elicited by protocol 4 conjunctive stimulation. (**b–e**) Similar to Fig. 17.2b–e, but for conjunction protocol 4, where 5PF stimulation and one depolarizing pulse were applied conjunctively at 0.5 Hz for 3 min under voltage-clamp conditions. In (**e**), * $p < 0.05$, ** $p < 0.01$, *t*-test

et al., 2000). When Gö6976 (0.3 μM) was contained in the internal solution, the EPSC amplitude after conjunctive stimulation failed to exhibit LTD in WT PCs either with protocol 2 (105.0 ± 1.7%, $n = 4$, $p = 0.06$, *t*-test) or 3 (97.7 ± 3.6%, $n = 3$, $p > 0.6$) (Fig. 17.8a, b). Hence, as far as the blocking effect of Gö6976 is concerned, the LTD induced by PF-Depo conjunctive stimulation is indistinguishable from that induced by PF-CF conjunctive stimulation. As tested with protocol 3, LTD was also blocked by Gö6976 in K882A PCs (98.5 ± 1.6%, $n = 3$, $p = 0.41$) and Δ7 PCs (99.7 ± 1.7%, $n = 3$, $p = 0.79$) (Fig. 17.7c, d). Hence, PKCα appears to play an essential role in LTD induction also in mutant PCs.

17.4 Discussion

17.4.1 Multiple Protocols for LTD Induction in Mutated Animal

C-terminus of GluA2 was essential for PKC-dependent internalization of AMPA-R containing GluA2, and LTD induction was believed to be impossible in PC expressing mutated GluA2 such as K882A and Δ7 (Steinberg et al., 2006). However, even in animals having these mutated GluA2, some modified protocols could actually

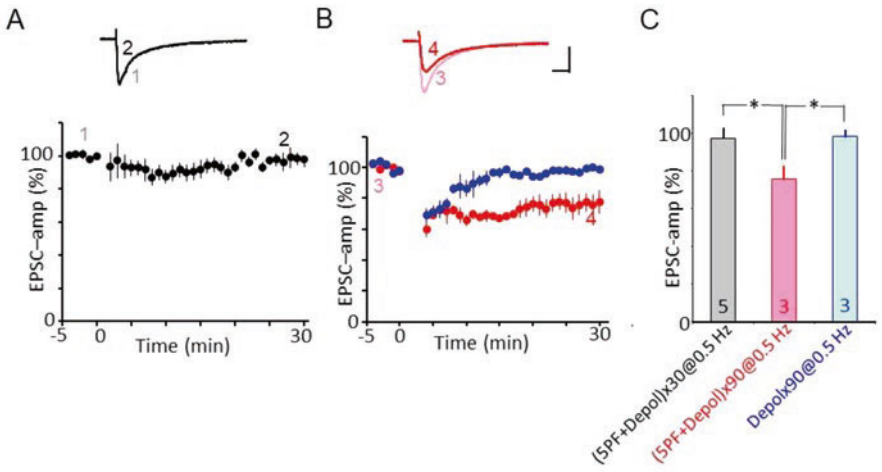

Fig. 17.7 Effect of number of repetitions of conjunctive stimulation on LTD induction by protocol 4. (**a**) Failure of LTD induction by protocol 4 conjunctive stimulation; repetition was 30 times at 0.5 Hz. Mean PF-EPSC amplitude recorded before and after protocol 4 conjunctive stimulation (black column at the bottom). Filled symbol indicates the mean EPSC amplitude. Inset: superimposed PF-EPSC traces (top) were recorded before (marked 1) and 25–29 min after conjunctive stimulation onset (marked 2). Each trace represents the average of six records. Bars: 100 pA, 10 ms. (**b**) Red symbol, LTD induced by protocol 4 conjunctive stimulation; blue symbol, no conjunction stimulation but somatic depolarization was applied 180 times at 0.5 Hz. LTD was not induced. Inset: superimposed PF-EPSC traces (top) were recorded before (marked 3) and 25–29 min after conjunctive stimulation onset (marked 4). Bars: 100 pA, 10 ms. (**c**) Summary plot of mean PF-EPSC amplitude recorded during 25–29 min after onset of conjunctive stimulation. Depol, depolarization. Numerical character in parentheses represents number of cells. ×30 = 30 times, ×90 = 90 times

induce LTD in PC (Yamaguchi et al., 2016). Compared to the simplest protocol, namely, simultaneous stimulation of PF and CF for 5 min at 1 Hz, other protocols were seemed to be more efficient to increase $(Ca^{2+})_{in}$. Thus, some compensated mechanism working in these mutant animals seemed to require higher $(Ca^{2+})_{in}$. Thus, compensatory mechanism of LTD in these mutants might be different from the ordinal molecular mechanism of LTD. However, this compensatory mechanism was indicated to be dependent on PKCα activity as in WT mice, because the selective PKCα inhibitor Gö6976 effectively blocked LTD induction in these mutant mice and WT mice (Fig. 17.5b). It may be that the stronger activation of PKCα by Ca^{2+} drives the downstream molecular machinery that may be modified by functional compensation for the mutations. The mechanism of such compensation is yet to be explored. The simplest possibility would be compensation by GluA3. Note that AMPAR at the PF-PC synapse consists of GluA2 and GluA3 subtypes (Srivastava et al., 1998) and that the GluR3 expression level is normal even in K882A and Δ7 mice (Steinberg et al., 2006). Note also that the GluA3 C-terminus can bind to GRIP/ABP and PICK1 (Bredt & Nicoll, 2003). Suppression of binding between the GluA3 C-terminus and GRIP/ABP through phosphorylation of Ser at

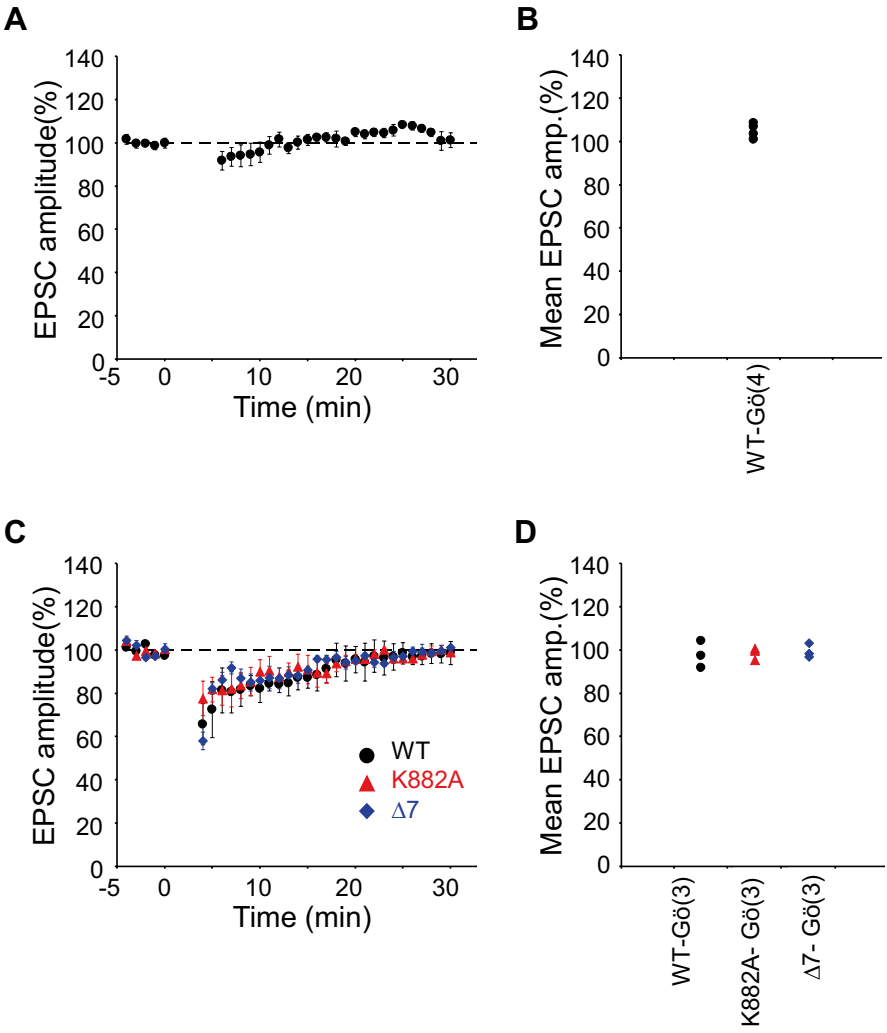

Fig. 17.8 Effects of PKCα blocker on LTD induction. (**a**) Similar to Fig. 17.2b, but obtained under infusion of Gö6976 with protocol 2 in WT mice. (**b**) Summary plot of mean PF-EPSC amplitude recorded during 25–29 min after onset of conjunctive stimulation in WT mice. (**c**) Similar to Fig. 17.5b–d, but obtained with protocol 3 under infusion of Gö6976 in WT, K882A, or Δ7 PCs. (**d**) No significant difference was found in the mean EPSC amplitude between before and after conjunctive stimulation in all three groups ($p > 0.05$, paired t-test)

the C-terminus by PKCα seems plausible because the 4-amino-acid sequence at the C-terminus of GluA3 is identical to that of GluA2, including the Ser site. It is interesting to determine whether phosphorylation of Ser at the C-terminus of GluA3 in these mutant mice requires a higher concentration of activated PKCα, just as LTD needs a stronger conjunctive stimulation in these mutant mice. In cultured PCs, even

a strong conjunctive stimulation did not induce LTD in cells from K882A or Δ7 mice (Steinberg et al., 2006). The extent of compensation by GluA3 might be low in cultured PCs. Also, compensation by GluA3 might depend on age, because PC in cerebellar slices from young K882A and Δ7 mice (P20–25) showed no LTD even after conjunction of high-frequency PF stimulation and somatic depolarization (0.5 Hz, 1 min) using a Cs^+-containing electrode. However, a similar but longer conjunctive stimulation (3 min) effectively induced LTD in elder mutant mice (3–6 months) (Fig. 17.4).

Compensation in K882A and Δ7 mutant mice might involve scaffold molecules in addition to GRIP1/2 for maintaining GluA2 at the postsynaptic density (PSD). Transmembrane AMPAR regulatory proteins (TARPs) are candidate molecules that deserve attention. In TARP γ-2 (stargazin) gene knockout mice, the content of GluA2 and GluA3 in synaptosome and PSD fractions is markedly reduced, suggesting the involvement of TARPs in the control of AMPAR surface expression at PF-PC synapses (Nomura et al., 2012). TARP γ-2, which is highly phosphorylated in its basal state, was dephosphorylated during chemically induced LTD in cerebellar slices (Yamazaki et al., 2015). The neuronal activity-dependent dephosphorylation of TARP γ-2 by calcineurin was indispensable for cerebellar LTD. Furthermore, PC-specific conditional deletion of TARP γ-2 with a γ-7 KO background impaired motor behaviors. Both GRIP1/2 and TARPs might be involved in stabilization of GluA2/3-containing AMPAR, and dissociation of GluA2/3 from them through direct or indirect action of PKCα might underlie LTD. However, the link between PKCα activation and the dissociation of GluA2/3 from TARP is missing.

An important conclusion from the present results is that LTD remains inducible in the mutants as far as the intensity of conjunctive stimulation is sufficiently increased. Hence, there is no reason to assume that LTD does not occur when these mutants perform motor learning. In this sense, the present results support the Marr-Albus-Ito hypothesis.

17.4.2 Roles of Other Synaptic Plasticities in the Cerebellar Cortex

In the cerebellar cortex, multiple forms of synaptic plasticity at different sites are induced during procedural memory formation (Fig. 17.1) (Gao et al., 2012). In addition to LTD at PF-PC synapse, other several types of synaptic plasticities are reported, such as spike-timing-dependent plasticity (STDP) at mossy fiber (MF)-granule cell (GrC), CF activity-dependent LTP at stellate cell to PC synapse, LTP at PF-PC synapse, and rebound potentiation of basket cell to PC synapse. Roles of these plasticities in motor learning are discussed here.

At the cerebellum input stage, STDP was reported between MF and GrC synapse (Sgritta et al., 2017). This type of synaptic plasticity may take part in cerebellar

receptive field reshaping after sensory stimulation. However, there seems no direct feedback signal from the motor performance; thus, this STDP at MF-GrC synapse would be difficult to directly contribute to the motor learning by correcting wrong performance, rather than contributing to fine-tuning of sensory and motor inputs.

As for inhibitory input to PC, GABA-mediated inhibitory synaptic transmission undergoes a long-lasting "rebound potentiation (RP)" after the activation of excitatory CF inputs (Kano et al., 1996). CF activity increases $(Ca^{2+})_{in}$ in PC, and activated Ca^{2+}/calmodulin-dependent protein kinase II (CaMKII), which causes structural alteration of $GABA_AR$-associated protein (GABARAP), subsequently enhances interaction between GABARAP and $GABA_AR$ γ2 subunit and shows RP by increasing $GABA_AR$ expression at the inhibitory synaptic site (Kawaguchi & Hirano, 2007). Expression of an inhibitory peptide, which blocks interaction between GABARAP and $GABA_AR$, selectively in PC impairs RP and VOR-adaptation, but not OKR adaptation (Tanaka et al. 2013). The RP obviously had feedback signal from motor performance through CF. Differences between LTD and RP are the following: first, RP is induced in all PC belonging to the same microzone, which is innervated by the same CF (Andersson & Oscarsson, 1978). The number of PCs belonging to one microzone was estimated from number of PCs which synchronously increase $[Ca^{2+}]_{in}$ at the firing of complex spike activated by the same climbing fiber, and estimated number was up to 30 (Ghosh et al., 2013). Thus, the rough number of PC in 1 microzone is considered around 30. Induction of LTD requires combined activities of CF and PF; thus, the number of PC expressing LTD should be far less than microzone size, which should correspond to PC pool size expressing RP simultaneously. Second, RP is induced without regarding the PF activity, which is conveying spatiotemporal pattern of sensory information and motor commands. So, we can in one IO cell, most of PC belonging to this CF's microzone would express RP, and only a small number of PC would express LTD. Surely RP could contribute to the motor learning, because it depends on CF-activity which conveys error signals of motor performance. However, comparing to the LTD, motor learning aquired through RP would be coarse, and RP might contribute at the early stage of learning of a complicated motor performance.

Repetitive stimulation of PF alone at low frequency causes potentiation of PF-PC EPSP (Sakurai, 1987). This postsynaptic type of LTP can reset LTD, and vice versa, LTD can reset LTP; thus, LTP and LTD mutually counterbalance each other (Lev-Ram et al. 2003). LTP of PF-PC synapse is mediated by NO (Lev-Ram et al., 2002), NSF (Kakegawa & Yuzaki 2005), and PP2B (Schonewille et al., 2010). Purkinje cell-selective deletion of PP2B abolishes postsynaptic LTP, whereas LTD was unaffected. The mutants showed impaired "gain-decrease" and "gain-increase" adaptation of VOR (Schonewille et al., 2010). In adaptation of VOR, where relatively small number of PC is involved and the same pool of PCs are engaged in new adaptation, old internal model should be reset by LTP to acquire new internal model.

17.4.3 Significance of LTD in Human Behavior

The significance of cerebellar LTD in motor learning was demonstrated in various mammals; however, significance of LTD in human motor learning is elusive. However, some circumstantial evidences suggested a crucial importance of LTD, compared to other types of synaptic plasticity in the cerebellar cortex. Recently, autoantibodies against neuronal surface proteins such as receptors and ion channels are known to cause neurological symptoms (Lancaster & Dalmau, 2012). However, autoantibodies associated with cerebellar ataxia have different feature from those associated with limbic encephalitis. In limbic encephalitis, anti-NMDA receptor and anti-LGI1 are often detected. LGI1 is important to express and localize voltage-dependent K channel (Kv1) (Hivert et al., 2019), and LGI1 enhanced Kv1 activity (Zhou et al., 2018). Kv1 and LGI1 are expressed in cerebellar neurons; however, association with anti-LGI1 antibody and cerebellar ataxia is rare (Mitoma et al., 2020). Also, NMDA-Rs distribute in cerebellar neurons, and NMDA-R of GrC was indicated to be essential for STDP at the synapse between MF and GrC (Sgritta et al., 2017), but association with immune-mediated cerebellar ataxia is not documented (Mitoma et al., 2020). On the other hand, immune-mediated cerebellar ataxia is associated with anti-mGluR1, anti-GluR delta 2, and anti-voltage-gated Ca channel (VGCC). Association of these autoantibodies with autoimmune limbic encephalitis is not documented (Mitoma et al., 2020). Target surface proteins of these three antibodies are essential to induce LTD in PC. The neuronal circuitry of the mature cerebellum stores acquired parameters of successful coordinated movements, and these internal models are essential for controlling the movement of the body parts without the need for sensory feedback (Ito, 2005, 2008). Acquired internal model would be routinely reset by LTD, in order to adapt to change in internal and external environment. Even if NMDA-R or K channel-related proteins are attacked by autoantibodies, as far as LTD remains normal, distortion of the internal model would be possibly recovered by LTD; however, if essential proteins for LTD induction are attacked by autoantibodies, there would be no way of recovery, and then symptom of cerebellar ataxia appears. As for the cerebellar cortex, PC is a final common output and LTD located at the final regulation step of PC output. Thus, LTD would play a crucial role in regulation of human movement.

References

Aiba, A., Kano, M., Chen, C., Stanton, M. E., Fox, G. D., Herrup, K., Zwingman, T. A., & Tonegawa, S. (1994). Deficient cerebellar long-term depression and impaired motor learning in mGluR1 mutant mice. *Cell, 79*, 377–388.

Albus, J. S. (1971). A theory of cerebellar function. *Mathematical Biosciences, 10*, 25–61.

Andersson, G., & Oscarsson, O. (1978). Climbing fiber microzones in cerebellar vermis and their projection to different groups of cells in the lateral vestibular nucleus. *Experimental Brain Research, 15*, 565–579.

Bredt, D. S., & Nicoll, R. A. (2003). AMPA receptor trafficking at excitatory synapses. *Neuron, 40*, 361–379.

De Schutter, E., & Bower, J. M. (1994). An active membrane model of the cerebellar Purkinje cell II. Simulation of synaptic responses. *Journal of Neurophysiology, 71*, 401–419.

De Zeeuw, C. I., Hansel, C., Bian, F., Koekkoek, S. K., van Alphen, A. M., Linden, D. J., & Oberdick, J. (1998). Expression of a protein kinase C inhibitor in Purkinje cells blocks cerebellar LTD and adaptation of the vestibulo-ocular reflex. *Neuron, 20*, 495–508.

Eccles, J. C., Ito, M., & Szentagothai, J. (1967). *The cerebellum as a neuronal machine*. Springer.

Fukuda, J., Kameyama, M., & Yamaguchi, K. (1981). Breakdown of cytoskeletal filaments selectively reduces Na and Ca spikes in cultured mammal neurones. *Nature, 294*, 82–85.

Gao, Z., van Beugen, B. J., & De Zeeuw, C. I. (2012). Distributed synergistic plasticity and cerebellar learning. *Nature Reviews. Neuroscience, 13*, 619–635.

Ghosh, K. K., Burns, L. D., Cocker, E. D., Nimmerjahn, A., Ziv, Y., El Gamal, A., & Schnitzer, M. J. (2013). Miniaturized integration of a fluorescence microscope. *Nature Methods, 8*, 871–878.

Hartmann, J., Blum, R., Kovalchuk, Y., Adelsberger, H., Kuner, R., Durand, G. M., Miyata, M., Kano, M., Offermanns, S., & Konnerth, A. (2004). Distinct roles of Gαq and Gα11 for Purkinje cell signaling and motor behavior. *The Journal of Neuroscience, 24*, 5119–5130.

Hirano, T., & Ohmori, H. (1986). Voltage-gated and synaptic currents in rat Purkinje cells in dissociated cell cultures. *Proceedings of the National Academy Sciences of the USA, 83*, 1945–1949.

Hirono, M., Sugiyama, T., Kishimoto, Y., Sakai, I., Miyazawa, T., Kishio, M., Inoue, H., Nakao, K., Ikeda, M., Kawahara, S., Kirino, Y., Katsuki, M., Horie, H., Ishikawa, Y., & Yoshioka, T. (2001). Phospholipase Cβ4 and protein kinase Cα and/or protein kinase CβI are involved in the induction of long term depression in cerebellar Purkinje cells. *The Journal of Biological Chemistry, 276*, 45236–45242.

Hivert, B., Marien, L., Agbam, K. N., & Faivre-Sarrailh, C. (2019). ADAM22 and ADAM23 modulate the targeting of the Kv1 channel-associated protein LGI1 to the axon initial segment. *Journal of Cell Science, 132*, jcs219774.

Ito, M., Sakurai, M., & Tongroach, P. (1982). Climbing fibre induced depression of both mossy fibre responsiveness and glutamate sensitivity of cerebellar Purkinje cells. *The Journal of Physiology, 324*, 113–134.

Ito, M. (2005). Bases and implications of learning in the cerebellum — Adaptive control and internal model mechanism. *Progress in Brain Research, 148*, 95–109.

Ito, M. (2008). Control of mental activities by internal models in the cerebellum. *Nature Reviews. Neuroscience, 9*, 304–313.

Kakegawa, W., Katoh, A., Narumi, S., Miura, E., Motohashi, J., Takahashi, A., Kohda, K., Fukazawa, Y., Yuzaki, M., & Matsuda, S. (2018). Optogenetic control of synaptic AMPA receptor endocytosis reveals roles of LTD in motor learning. *Neuron, 99*, 985–998.

Kakegawa, W. & Yuzaki, M. (2005) A mechanism underlying AMPA receptor trafficking during cerebellar long-term potentiation. *Proceedings of the National Academy Science of the USA. 102*. 17846–17851.

Kano, M., Kano, M., Fukunaga, K., & Konnerth, A. (1996). Ca^{2+}-induced rebound potentiation of γ-aminobutyric acid-mediated currents requires activation of Ca^{2+}/calmodulin-dependent kinase II. *Proceedings of the National Academy Sciences of the USA, 93*, 13351–13356.

Karachot, L., Kado, R. T., & Ito, M. (1994). Stimulus parameters for induction of long-term depression in in vitro rat Purkinje cells. *Neuroscience Research, 21*, 161–168.

Kashiwabuchi, N., Araki, K., Hirano, T., Shibuki, K., Takayama, C., Inoue, Y., Kutsuwada, T., Yagi, T., Kang, Y. N., Aizawa, S., & Mishina, M. (1995). Impairment of motor coordination, Purkinje cell synapse formation, and cerebellar long-term depression in GluRδ2 mutant mice. *Cell, 81*, 245–252.

Kawaguchi, S., & Hirano, T. (2007). Sustained structural change of $GABA_A$ receptor-associated protein underlies long-term potentiation at inhibitory synapses on a cerebellar Purkinje neuron. *The Journal of Neuroscience, 27*, 6788–6799.

Kishimoto, Y., Hirono, M., Sugiyama, T., Kawahara, S., Nakao, K., Kishio, M., Katsuki, M., Yoshioka, T., & Kirino, Y. (2001). Impaired delay but normal trace eye blink conditioning in PLCβ4 mutant mice. *Neuroreport, 17*, 2919–2922.

Koekkoek, S. K. E., Yamaguchi, K., Milojkovic, B. A., Dortland, B. R., Ruigrok, T. J. H., Maex, R., De Graaf, W., Smit, A. E., Werf, F. V., Bakker, C. E., Willemsen, R., Ikeda, T., Kakizawa, S., Onodera, K., Nelson, D. L., Mientjes, E., Joosten, M., De Schutter, E., Oostra, B. A., Ito, M., & De Zeeuw, C. L. (2005). Deletion of *FMR1* in Purkinje cells enhances parallel fiber LTD, enlarges spines, and attenuates cerebellar eyelid conditioning in fragile X syndrome. *Neuron, 47*, 339–352.

Katoh, A., Yoshida, T., Himeshima, Y., Mishina, M. & Hirano, T. (2005). Defective control and adaptation of reflex eye movements in mutant mice deficit in either the glutamate receptor delta2 subunit or Purkinje cells. *European Journal of Neuroscience, 21*, 1315–1326.

Kohda, K., Kakegawa, W., Matsuda, S., Yamamoto, T., Hirano, H., & Yuzaki, M. (2013). The δ glutamate receptor gates long-term depression by coordinating interactions between two AMPA receptor phosphorylation sites. *Proceedings of the National Academy Sciences of the USA, 110*, E948–E957.

Lancaster, E., & Dalmau, J. (2012). Neuronal autoantigens-pathogenesis, associated disorders and antibody testing. *Nature Reviews. Neurology, 8*, 380–392.

Lev-Ram, V., Wong, S. T., Storm, D. R., & Tsien, R. Y. (2002). A new form of cerebellar long-term potentiation is postsynaptic and depends on nitric oxide but not cAMP. *Proceedings of the National Academy Sciences of the USA, 99*, 8389–8393.

Lev-Ram, V., Mehta, S. B., Kleinfeld, D., & Tsien, R. Y. (2003). Reversing cerebellar long-term depression. *Proceedings of the National Academy Sciences of the USA, 100*, 15989–15993.

Linden, D. J., & Connor, J. A. (1991). Participation of postsynaptic PKC in cerebellar long-term depression in culture. *Science, 254*, 1656–1659.

Marr, D. (1969). A theory of cerebellar cortex. *The Journal of Physiology, 202*, 437–470.

Masugi-Tokita, M., Tarusawa, E., Watanabe, M., Molnár, E., Fujimoto, K., & Shigemoto, R. (2007). Number and density of AMPA receptors in individual synapses in the rat cerebellum as revealed by SDS-digested freeze-fracture replica labeling. *The Journal of Neuroscience, 27*, 2135–2144.

Mitoma, H., Honnorat, J., Yamaguchi, K., & Manto, M. (2020). Fundamental mechanisms of autoantibody-induced impairments on ion channels and synapses in immune-mediated cerebellar ataxias. *International Journal of Molecular Sciences, 21*, 4936.

Miyata, M., Kim, H. T., Hashimoto, K., Lee, T. K., Cho, S. Y., Jiang, H., Wu, Y. P., Jun, K., Wu, D. Q., Kano, M., & Shin, H. S. (2001). Deficient long-term synaptic depression in the rostral cerebellum correlated with impaired motor learning in phospholipase Cβ4 mutant mice. *The European Journal of Neuroscience, 13*, 1945–1954.

Nomura, T., et al. (2012). Cerebellar long-term depression requires dephosphorylation of TARP in Purkinje cell. *The European Journal of Neuroscience, 35*, 402–410.

Sakurai, M. (1987). Synaptic modification of parallel fibre-Purkinje cell transmission in *in vitro* guinea-pig cerebellar slices. *The Journal of Physiology, 394*, 463–480.

Schonewille, M., Belmeguenai, A., Koekkoek, S. K., Houtman, S. H., Boele, H. J., van Beugen, B. J., Gao, Z., Badura, A., Ohtsuki, G., Amerika, W. E., Hosy, E., Hoebeek, F. E., Elgersma, Y., Hansel, C., & De Zeeuw, C. I. (2010). Purkinje cell-specific knockout of the protein phosphatase PP2B impairs potentiation and cerebellar motor learning. *Neuron, 67*, 618–628.

Schonewille, M., Gao, Z., Boele, H. J., Veloz, M. F. V., Amerika, W. E., Simek, A. A. M., De, J. M. T., Steinberg, J. P., Takamiya, K., Hoebeek, F. E., Linden, D. J., Huganir, R. L., De Zeeuw, C. I., & CI. (2011). Reevaluating the role of LTD in cerebellar motor learning. *Neuron, 70*, 43–50.

Srivastava, S., Osten, P., Vilim, F. S., Khatri, L., Inman, G., States, K. B., Daly, C., DeSouza, S., Abagyan, R., Valtschanoff, J. G., Weinberg, R. J., & Ziff, E. B. (1998). Novel anchorage of GluR2/3 to the postsynaptic density by the AMPA receptor–binding protein ABP. *Neuron, 21*, 581–591.

Steinberg, J. P., Takamiya, K., Shen, Y., Xia, J., Rubio, M. E., Yu, S., Jin, W. Y., Thomas, G. M., Linden, D. J., & Huganiret, R. L. (2006). Targeted in vivo mutations of the AMPA receptor subunit GluR2 and its interacting protein PICK1 eliminate cerebellar long-term depression. *Neuron, 49*, 845–860.

Sgritta, M., Locatelli, F., Soda, T., Prestori, F., & D'Angelo, E. U. (2017). Hebbian spike-timing dependent plasticity at the cerebellar input stage. *The Journal of Neuroscience, 37*, 2809–2823.

Swensen, A. M., & Bean, B. (2003). Ionic mechanisms of burst firing in dissociated Purkinje neurons. *Journal of Neuroscience, 23*(29), 9650–9663.

Tanaka, S., Kawaguchi, S., Shioi, G., & Hirano, T. (2013). Long-term potentiation of inhibitory synaptic transmission onto cerebellar Purkinje neurons contributes to adaptation of vestibulo-ocular reflex. *The Journal of Neuroscience, 33*, 17209–17220.

Wang, S. S., Denk, W., & Hausser, M. (2000). Coincidence detection in single dendritic spines mediated by calcium release. *Nature Neuroscience, 3*, 1266–1273.

Wang, Y. T., & Linden, D. J. (2000). Expression of cerebellar long-term depression requires post-synaptic clathrin-mediated endocytosis. *Neuron, 25*, 635–647.

Xia, J., Chung, H. J., Wihler, C., Huganir, R. L., & Linden, D. J. (2000). Cerebellar long-term depression requires PKC-regulated interactions between GluR2/3 and PDZ domain–containing proteins. *Neuron, 28*, 499–510.

Yamaguchi, K., Itohara, S., & Ito, M. (2016). Reassessment of long-term depression in cerebellar Purkinje cells in mice carrying mutated GluA2 C terminus. *Proceedings of the National Academy Sciences of the USA, 113*, 10192–10197.

Yamazaki, M., Le Pichonc, C. E., Jacksona, A. C., Cerpasa, M., Sakimurab, K., Scearce-Leviec, K., & Nicoll, R. A. (2015). Relative contribution of TARPs γ-2 and γ-7 to cerebellar excitatory synaptic transmission and motor behavior. *Proceedings of the National Academy Sciences of the USA, 112*, E371–E379.

Zhou, L., Zhou, L., Su, L. D., Cao, S. L., Xie, Y. J., Wang, N., Shao, C. Y., Wang, Y. N., Zhou, J. H., Cowell, J. K., & Shen, Y. (2018). Celecoxib ameliorates seizure susceptibility in autosomal dominant lateral temporal epilepsy. *The Journal of Neuroscience, 38*, 3346–3357.